INSTABILITIES AND SPACE CHARGE*

M. Blaskiewicz†, K. Mernick
BNL, Upton, NY 11973, USA

Abstract

The coherent stability problem for proton and heavy ion beams is reviewed. For all but the highest energies space charge is the dominant coherent force. While space charge alone appear benign its interaction with other impedances is less clear. The main assumptions used in calculations and their justifications will be reviewed. Transverse beam transfer function data from RHIC will be used to compare theory and experiment and some pitfalls will be discussed.

MODELING THE TRANSVERSE FORCE

The effect of space charge on longitudinal instabilites goes back to early work on the negative mass instability [1]. Early work on coasting beam transverse instabilities included the effect of space charge as well [2]. Both these treatments used a leading order approximation with a longitudinal force proportional to the derivative of the instantaneous current and a transverse force

$$F_x = \kappa I(\tau)[x - \bar{x}(\tau,t)] \qquad (1)$$

where τ is the particle arrival time with respect to the synchronous particle, t is time, $I(\tau)$ is the instantaneous current, x is the transverse coordinate and $\bar{x}(\tau,t)$ is the transverse centroid position as a function of longitudinal coordinate and time. The constant κ depends on the beam radius. There are several assumptions [3]:

1. The fields are electrostatic in the comoving frame.
2. The wavelength of perturbations in the comoving frame are long compared to the beam radius.
3. The unperturbed transverse distribution is KV, resulting in a constant density within the beam at a given τ.
4. First order perturbation theory is used.
5. The fields due to boundary conditions are neglected.

For small perturbations the nonlinearities due to images do not depend on the beam dynamics and will be subsumed in a generic octupolar force. For direct space charge actual beams are generally not KV and the accuracy of Eq. (1) has been studied in [4–8] within the context of coasting beams. It was found that the nonlinearity due to direct space charge is relevant only when other forms of damping are present. Space charge enhances damping due to lattice nonlinearity if the betatron tune increases with betatron amplitude. Changing the sign results in less damping that without space charge. The tune shift with amplitude due to short strong quadrupoles has the right sign and works in both planes [9].

Figures 1 and 2 show threshold diagrams where ΔQ_0 is the complex tune shift an undamped beam would have.

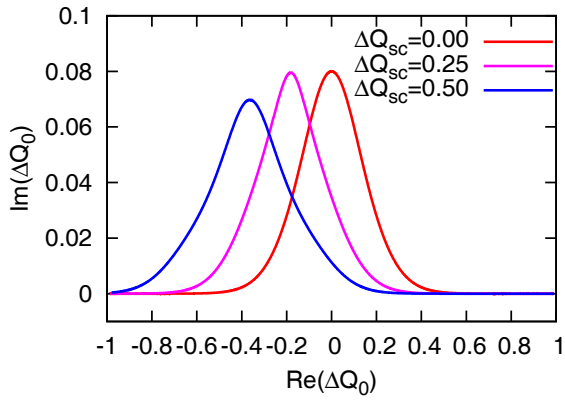

Figure 1: Threshold diagrams for tune spread due to chromatic tune spread with space charge. Average space tune shifts are quoted and the rms chromatic tune spread is 0.1.

Stable tune shifts for damped beams are below the curves. The unperturbed transverse action distribution is $F_0(J) = (3/J_0)(1 - J/J_0)^2$ and space charge is modeled as an interparticle force containing linear and cubic terms [3]. The ratio of the tune spread to the average tune shift matches that for a round gaussian beam. These solutions are for one dimensional motion and the expresion for the theshold impedance as a function of coherent beam tune is a rational function of three different dispersion integrals [5][Eq. (31)]. As is clear from the plots these effects are important if true and we go on to test them with particle tracking.

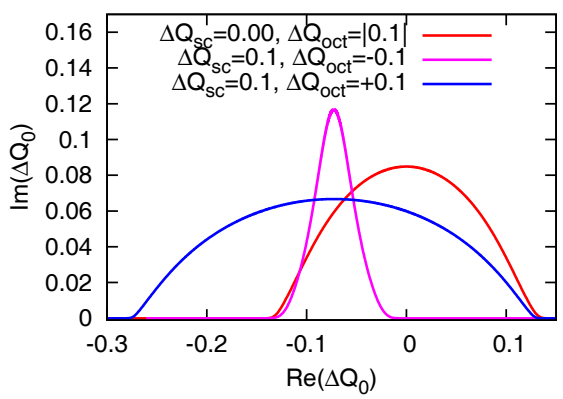

Figure 2: Threshold diagrams for tune spread due to octupoles with space charge. Average space charge and octupolar tune shifts are quoted and a chromatic tune spread of 0.01 is also included.

When both transverse dimensions are included and the space charge is modeled more accurately, certain forms of

* Work performed under the auspices of the United States Department of Energy
† blaskiewicz@bnl.gov

ISBN 978-3-95450-173-1

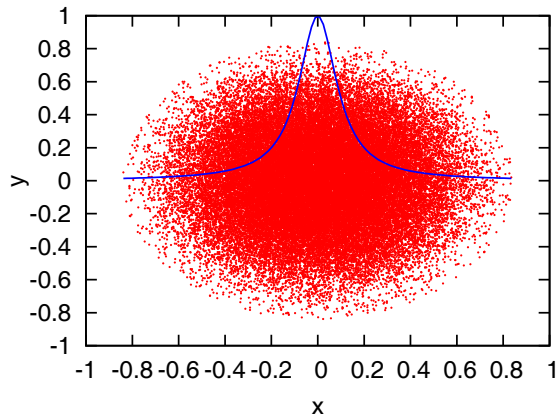

Figure 3: Initial particle distribution and space charge smoothing function used in simulations. 50,000 particles were tracked. Increasing the number of particles by a factor of 5 and increasing the update rate by a factor of 5 had no significant impact.

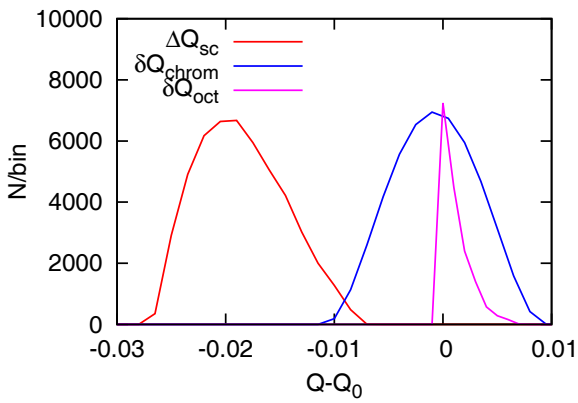

Figure 4: Tune distributions used in the tracking.

the dispersion relation have been conjectured [4, 7, 8] but reliable solutions appear to require tracking. Consider the simple model

$$\frac{dp_{xj}}{d\theta} + Q_x x_j = C_o x_j (x_j^2 + p_{xj}^2) - \delta Q_j x_j + C_{sc} \sum_{m=1}^{N_p} \frac{x_j - x_m}{\epsilon^2 + (x_j - x_m)^2 + (y_j - y_m)^2} + \frac{2}{N_p} \sum_{m=1}^{N_p} Im(\Delta Q_0) p_{xm} - Re(\Delta Q_0) x_m \quad (2)$$

$$\frac{dx_j}{d\theta} - Q_x p_{xj} = -C_o p_{xj} (x_j^2 + p_{xj}^2) + \delta Q_j p_{xj}. \quad (3)$$

In the first lines of Eq. (2) and (3) θ is the azimuth which increases by 2π each turn, Q_x is the bare horizontal tune, δQ_j is the chromatic tune shift for particle j and C_o characterizes the strength of the octupolar tune shift. In the second line of Eq. (2) C_{sc} characterizes the strength of the space charge force with smoothing length ϵ. The third line of Eq. (2) contains the impedance like forces. For no tune spread the beam centroid oscillates with real tune $Q_x + Re(\Delta Q_0)$ and grows in amplitude by $\exp[2\pi Im(\Delta Q_0)]$ each turn. The y direction has a different central tune and no ΔQ_0 terms.

Figure 3 shows inital particle distributions and the smoothing fucntion used in the space charge calculations. The initial phase space distribution was matched to $(1 - x^2 - y^2 - p_x^2 - p_y^2)^2$ and 50,000 particles were tracked with 30 updates per betatron oscillation. Increasing the number of particles to 250,000 or increasing the update rate to 150 updates per oscillation had no significant effect on collective modes. Before considering detuning with amplitude we focus on the simpler chromatic tune spreads. Figure 4 shows the tune distributions for chromaticity induced tune spread and space charge tune spread. Octupolar detuning will be considered later and initially we drop space charge also, yielding purely linear equations of motion. Figure 5 shows emittance as a function of time within the stability boundary for a beam with $Im(\Delta Q_0) = 0.0002$. The magenta curve has fractional emittance growth per turn $\exp(4\pi Im(\Delta Q_0)/N_p)$ and follows from a stochastic cooling model [10].

Figure 6 shows the observed growth rate as a function of the real tune shift induced by a wall impedance. The space charge force was evaluated using a fast fourier transform convolution algorithm with a 128 by 128 grid on the beam and a double up procedure to avoid image forces. The blue and red curves in Figure 6 are the similar but when more turns are tracked instabilites can occur later. This is shown in the magenta curve. It is clear that the tracking results do not show the increased region of stability shown in Figure 1. Simulations employing octupolar damping are shown in Figure 7. As is clear from the figure the threshold value of the wall impedance depends on the number of turns tracked. While there is generally a slow, secular increase in the transverse emittance the growth rates were from data before significant emittance growth occured. Both Figures 6 and 7 show behavior typical of extended tracking with space charge. If you wait long enough things almost always go unstable. This is clearly not physical since beams persist for hours at RHIC injection energies with space charge tune shifts far in excess of the synchrotron tune. Other machines, such as the BNL AGS, can have stable beams for seconds with space charge tune shifts of order 0.2. This presents us with something of an impasse. For short runs both Figures 6 and 7 show that space charge increases the range of the stable region beyond what would be expected for a reactive impedance while longer simulations show the reverse. To make some sort of headway for bunched beams we will assume that Equation (1) is sufficiently accurate for beams of interest. While vastly reducing the theoretical and computational complexity it should be clear that this is a fairly strong assumption and that the problem of a correct transverse force model is unresolved.

Exact solutions using Eq. (1) for transverse modes of a bunched beam with constant line density within the bunch are given in appendix II of [11]. Exact longitudinal modes

ISBN 978-3-95450-173-1

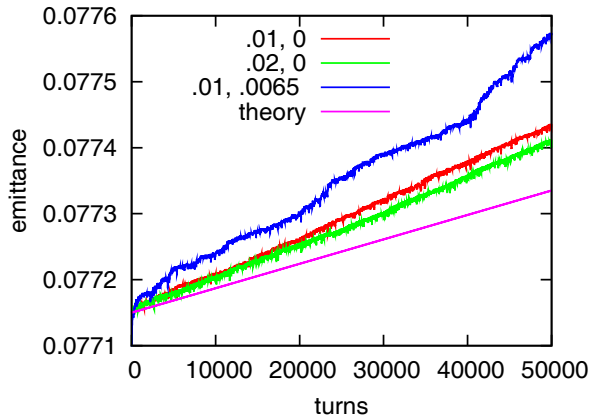

Figure 5: Emittance growth for purely linear simulations within the Vlasov stability boundary. The theory assumes all particles have imaginary tune $Im(\Delta Q_0)/N_p$ with perfect phase mixing. The blue curve is just inside the stability boundary.

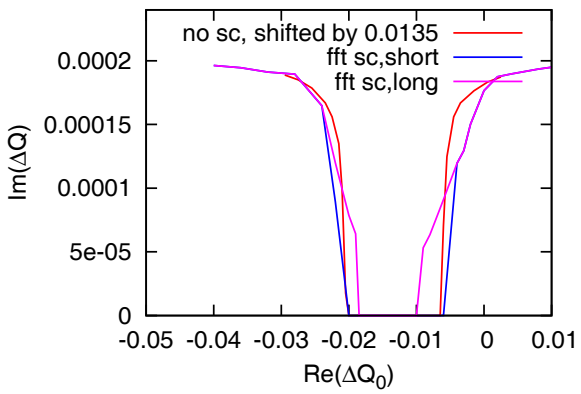

Figure 6: The imaginary part of the tune seen in tracking with damping due to chromatic tune spread or frequency spread. The blue cure is the result of tracking with realistic space charge for 5000 turns and the red curve is a shifted version from tracking with no space charge. The magenta curve was obtained for tracking for 50,000 turns, no significant secular changes in the beam were observed before the instability started.

for a bunch with a parabolic current profile are given in [12] which also reduces the dispersion relation to a polynomial. The problem can also be cast as a finite eigenvalue problem [13, 14]. In the exact solutions the forces due to space charge end up being linear in the sense that the depressed tunes are just numbers, not functions of the longitudinal coordinates. The effect of space charge on transverse instabilites with smooth longitudinal profiles was studied in [3, 13–21]. The mode expansion technique was shown to be suspect in [13, 14]. It is not clear how many of the conclusions of these studies are consistent and it is certainly true that the broad conclusions presented in [14] are contradicted by [21].

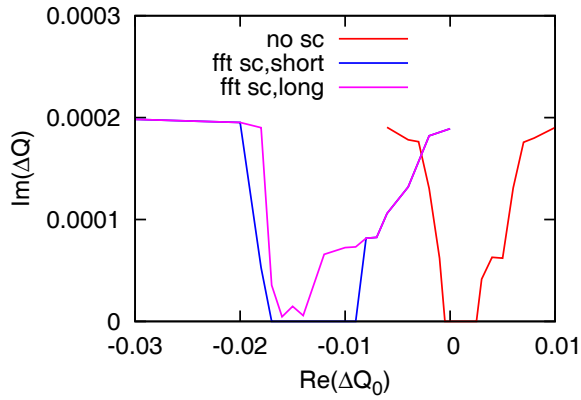

Figure 7: The imaginary part of the tune seen in tracking with damping due to octupolar tune spread. The blue cure is the result of tracking with realistic space charge for 5000 turns and the red curve is from tracking with no space charge. The magenta curve was obtained for tracking for up to 50,000 turns. Data were limitied to regions where no secular changes in the beam emittance were observed before the instability started.

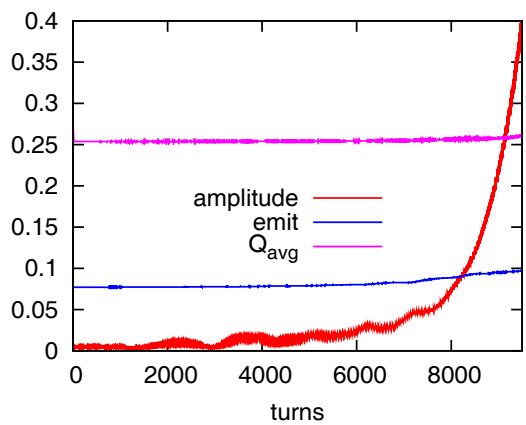

Figure 8: Simulation with octupolar tune spread and space charge. The points with $Re(\Delta Q_0) = -0.018$ in Figure 7 were obtained from this run. Turns 1000 though 5000 yielded $Im(Q) = 0.53\times10^{-4}$ while the last 1000 turns gave $Im(Q) = 1.9 \times 10^{-4}$.

In the next section we will present some beam transfer function data from RHIC in hope of providing some clarity

BEAM TRANSFER FUNCTIONS

A beam transfer function (BTF) is obtained when a kicker is driven at a single frequency and a pickup measures the phase and amplitue of the beam response at that same frequency. One steps through frequencies and maps out the beam response [22]. Figure 9 show vertical BTF data from RHIC for polarized protons at injection. The bunches were ~ 35 ns at base and the BTFs were take near 250 MHz. The two sidebands were taken on different days and in different rings. The peaks of the BTFs were fit with a parabolic cap.

ISBN 978-3-95450-173-1

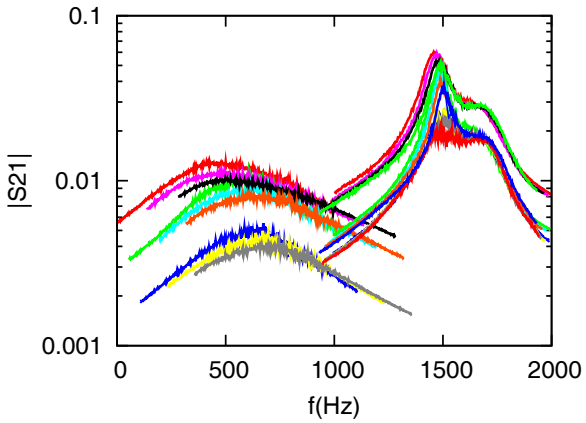

Figure 9: BTF data from RHIC near 250 MHz with protons at $\gamma = 25.5$. The average beam currents ranged from 0.3 to 1.5 A. Vertical data from the $n - Q$ sidband of the blue ring are on the left and data from the $n + Q$ vertical sideband of the yellow ring are offset to the right by 1 kHz.

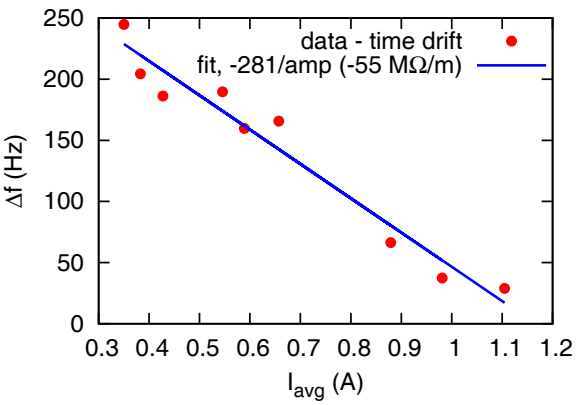

Figure 10: Frequency shift of $n - Q$ vertical sideband for the blue ring.

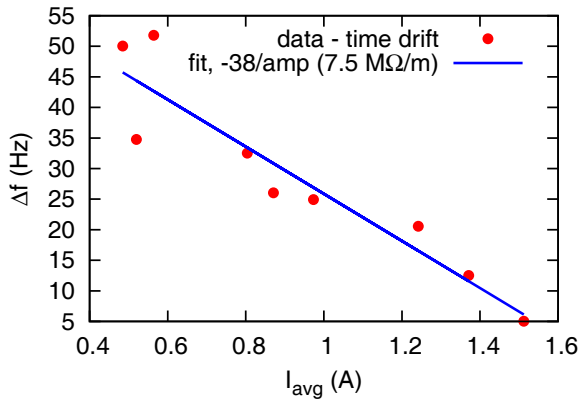

Figure 11: Frequency shift of $n + Q$ vertical sideband for the yellow ring.

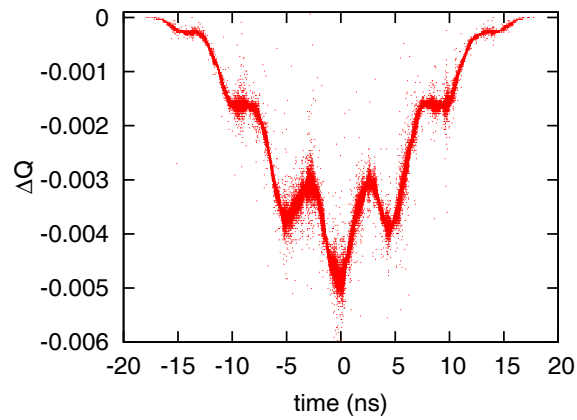

Figure 12: Space charge tune shift as a function of bunch postion used in the simulations for an average current of 1A. The multi-hump structure is due to the admixture of 9.4 MHz and 197 MHz rf voltage.

The frequency was assumed to be a linear function of intensity and a linear drift in time was allowed for. The fitting results for the two sidebands are shown in Figures 10 and 11.

The average current for a bunch is defined to be

$$I_{avg} = \frac{\int_{bunch} I^2(t)dt}{\int_{bunch} I(t)dt} \quad (4)$$

The simulations assume Equation (1) is sufficiently accurate. Given this assumption any representation of collective forces that leads to Equation (1) will be acceptable. Instead of using a KV distribution and demanding a small perturbation it is much faster and more accurate to take the force on particle j to be

$$F_j = C_{sc} \sum_{k=1}^{N_p} (x_j - x_k)\lambda(\tau_j - \tau_k) \quad (5)$$

where x_j and τ_j are the transverse and longitudinal coordinates of the particle kicked, and $\lambda(\tau)$ is a smoothing function. Care must be taken to keep the smoothing length small enough and the number of macroparticles (N_p) large enough. Figure 12 shows the incoherent space charge tune shift along the bunch and Figure 13 shows some simulated BTFs [23]. We were unable to reproduce the shoulder apparent in the $n + Q$ sideband of the data. Figures 14 and 15 show simulation results for frequency shift versus time. Agreement with the data is not good. One possible cause for the discrepancy is that the transverse emittance of the RHIC beam is a function of beam intensity. That would cause the space charge impedance to be a function of intensity. It is also likely that the broad band impedance is not the same in the two rings. Impedance measurements using kicked beams show differences by a factor of 2 [24]. We plan to take more data with both sidebands from each ring and to monitor and or control the transverse emittance.

ISBN 978-3-95450-173-1

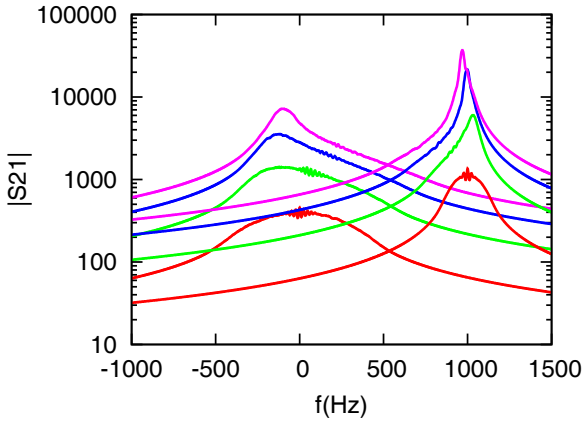

Figure 13: Simulated BTF with Z_{sc} = 44 MΩ/m and Z_{wall} = 5 MΩ/m. The average beam currents were 1, 0.66, 0.33, 0.10 A.

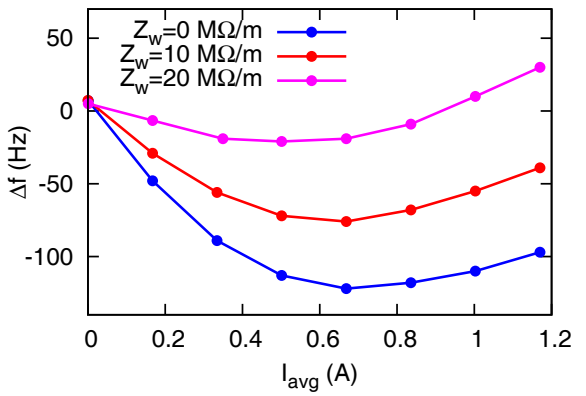

Figure 14: Simulated frequency shift of $n - Q$ vertical sideband.

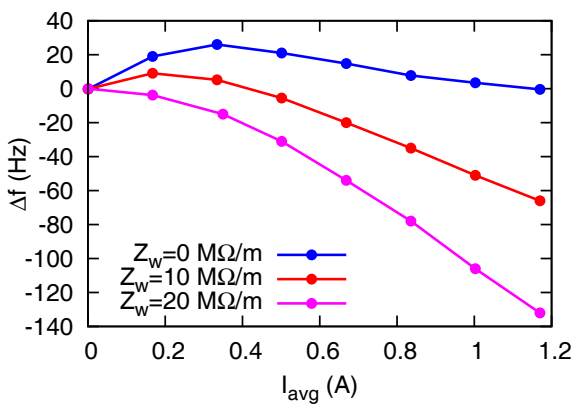

Figure 15: Simulated frequency shift of $n + Q$ vertical sideband.

REFERENCES

[1] C.E. Nielsen, A.M. Sessler Rev. Sci. Instr. Vol. 30, p80, (1959).

[2] L.J. Laslett, V.K. Neil, A.M. Sessler Rev. Sci. Instr. Vol. 36, No. 4, p436, (1965).

[3] M. Blaskiewicz, M.A. Furman, M. Pivi, R.J. Macek PRSTAB Vol. 6, 044203 (2003).

[4] D. Mohl, H. Schonauer, *Proc. IX Int. Conf. High Energy Acc.*, Stanford, (1974) (AEC, Washington, D.C. 1974) p. 380.

[5] M. Blaskiewicz PRSTAB Vol. 4, 044202 (2001).

[6] D.V. Pestrikov NIMA Vol. 578 p65 (2007).

[7] V. Kornilov, O. Boine-Frankenheim, I. Hofmann PRSTAB Vol. 11, 014201 (2008).

[8] A. Burov, V. Lebedev PRSTAB Vol. 12, 034201 (2009).

[9] R. Baartman, in*Proceedings of the Particle Accelerator Conference (PAC97), Vancouver, Canada* (IEEE, Piscataway, NJ, 1998), p. 1415.

[10] M. Blaskiewicz, J.M. Brennan Cool13

[11] F. Sacherer CERN/SI-BR/72-5 (1972)

[12] David Neuffer *Particle Accelerators* Vol. 11, p23, (1980).

[13] M. Blaskiewicz, W.T. Weng PRE Vol. 50, No. 5, p4030 (1994).

[14] M. Blaskiewicz PRSTAB Vol. 1, 044201 (1998).

[15] A. Burov PRSTAB Vol. 12, 044202 (2009); PRSTAB Vol. 12, 109901 (2009)

[16] V. Balbekov PRSTAB Vol. 12, 124402 (2009).

[17] J.A. Holmes, S. cousineau, v. Danilov, L. Jain PRSTAB Vol. 14, 074401 (2011).

[18] V. Balbekov PRSTAB Vol. 14, 094401 (2011).

[19] V. Balbekov PRSTAB Vol. 15, 054403 (2012).

[20] V. Kornilov, O. Boine-Frankenheim PRSTAB Vol. 15, 114201 (2012).

[21] M. Blaskiewicz IPAC2012 weppr097

[22] D. Boussard, CERN 87-03, p. 416, 1987.

[23] M. Blaskiewicz, V. Ranjbar NAPAC13 (2013).

[24] N. Biancacci *et.al.* IPAC2014 p1730 (2014).

ISBN 978-3-95450-173-1